



Direct methane solid oxide fuel cell working by gradual internal steam reforming: Analysis of operation

Jean-Marie Klein, Marc Hénault, Claude Roux, Yann Bultel, Samuel Georges*

Laboratoire d'Electrochimie et de Physico-chimie des Matériaux et des Interfaces – LEPMI, UMR 5631 CNRS-INPG-UJF, BP.75. 38402 Saint Martin d'Hères Cedex, France

ARTICLE INFO

Article history:

Received 16 October 2008

Received in revised form

13 November 2008

Accepted 25 November 2008

Available online 6 December 2008

Keywords:

SOFC

Internal reforming

Steam reforming

Methane

Energy

ABSTRACT

A solid oxide fuel cell was designed to be operated with pure hydrocarbons, without additive or carrier gas, in order to bring technological simplifications, cost reductions and to extend the fuel flexibility limits. The cell was built-up from a conventional cell (LSM/YSZ/Ni-YSZ), to which was added a Ir–CeO₂ catalyst layer at the anode side and an original current collecting system. The cell was first operated with steam in gradual internal reforming (GIR) conditions ($R = [\text{H}_2\text{O}]/[\text{CH}_4] < 1$) with carrier gas at the anode. The optimal operating parameters were determined in terms of flow rates, cell potential, and fuel utilisation. The cell was finally operated with pure dry methane at 900 °C at 0.6 V yielding current density of about 0.1 A cm⁻² at max power for 120 h. Small but abrupt deterioration of the performances was observed, but no carbon deposition. Electrical and chemical analysis of this degradation are provided.

At total, the fuel cell was operated for more than 200 h in pure dry methane, demonstrating that gradual internal reforming actually occurred efficiently in the anode compartment, which make possible operation without reforming agent such as H₂O or CO₂ for other hydrocarbon fuels.

© 2008 Elsevier B.V. All rights reserved.

1. Introduction

Solid oxide fuel cells can now operate with good efficiency and decent durability with hydrogen as the fuel at intermediate temperature (600–700 °C), even though technological efforts still have to be made in order to stretch life time and reduce fabrication, operation and recycling costs. Given the actual energetic context, and in particular the aspects concerning production, storage and distribution infrastructures of hydrogen, the use of other fuels based on hydrocarbons sounds interesting to be considered for the next decades.

Natural gas, bio-gas, waste fuels, bio-ethanol or other sources are interesting candidates for clean and cheap operation of various devices like SOFC, instead of oil-based fuels in the future. In this context, several solutions have been proposed to overcome technical issues and enable direct and stable hydrocarbon operation of SOFC without coke formation [1].

It was demonstrated that for operation with humidified (3%) methane of a fuel cell involving conventional Ni-YSZ anode, critical current density had to be reached to avoid carbon cracking and to maintain stable operation for several hours [2]. A cell was operated for 168 h in humidified methane at 0.6 V, $J = 0.8 \text{ A cm}^{-2}$ and 700 °C. Moreover, it was observed that this critical value increased with temperature because of the increase of methane cracking rate

above 700 °C. These observations point out the relation between the O²⁻ flow rate through the electrolyte and the problems of coking on the anodic electro-catalytic sites. The group of Barnett then introduced the concept of inert or catalytically active layer added at the anode side [3] and acting as either physical barrier or catalytic membrane. Good performances were obtained using these concepts for dry (CO₂) reforming of iso-octane [3] and for partial oxidation of methane using methane–air mixtures by several groups [4,5], which emphasises the essential role of heterogeneous catalysis in the operation of such fuel cells with hydrocarbons.

As another alternative, direct electrochemical oxidation of gaseous or liquid hydrocarbons has been successfully attempted [6–8] using Cu–CeO₂-YSZ composite anodes. Ceria presents high activity for hydrocarbons oxidation, while Cu, unlike metallic Ni of Ni-YSZ cermets, does not promote C–H bond activation, so that carbon formation is avoided. The addition of precious metals (Pd, Pt, Rh) led to an increase of the catalytic activity of the anode, yielding improved performances, especially when CH₄ was used as the fuel [9].

These researches demonstrated that solid oxide fuel cells could be operated with hydrocarbons without carbon cracking for several hundreds of hours. More work is now needed to improve the systems and extend life time, but the feasibility is henceforth established.

However, in the experimental studies mentioned above, the fuels were always consisted of several gas as steam, air or carbon dioxide added to the hydrocarbon, because the reactions involved or aimed at being involved by the authors (steam reforming, partial

* Corresponding author.

E-mail address: samuel.georges@lepmi.inpg.fr (S. Georges).

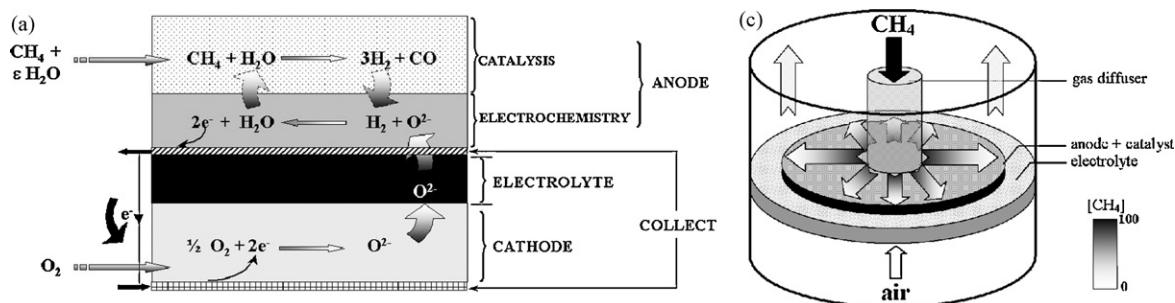
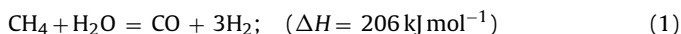


Fig. 1. (a) Principle of gradual internal reforming (GIR) associated with the anodic catalytic membrane; (b) sketch showing the applicability of the concept of GIR to a planar test-cell.

oxidation or dry reforming) necessitated to introduce a specific reactant at the anode inlet. On the contrary, operation of SOFC with hydrocarbons will be most interested from technological and economical points of view, with pure hydrocarbons as the fuel. Stable and long-term operation of a fuel cell with a single gas without additive or carrier gas will be the best demonstration of fuel flexibility and will open the way for the use of various fuels, extending the applicability of SOFCs. Accordingly, the aim of this study was to demonstrate that a conventional solid oxide fuel cell, involving state of the art materials, can be operated with pure and dry hydrocarbons without any additive in middle-term laboratory experiments without dramatic performances deterioration or carbon cracking. The reaction to be aimed at occurring in our experiments is steam reforming:



This feature is achieved by addition of a catalyst layer onto the anode, and by the design of an original internal collecting system. With this architecture, the cell will operate in gradual internal reforming (GIR) conditions. This concept was first proposed by Vernoux et al. [10].

GIR operation will be associated with the catalytically active layer so that catalytic and electrochemical reactions will be separated. This separation allows the application of the best materials for each function.

Encouraging experimental tests have already been reported [11,12] for tubular and planar configurations. This paper provides an accurate characterisation of the middle-term operation of a fuel cell that presents this original architecture. Electrical and electrochemical behavior of the cell is analyzed as well as outlet gas phase composition as a function of time. Both data are related to determine the reasons of the cell partial deactivation after 120 h. On original current collecting system is also presented.

The principle of gradual internal reforming of methane, associated with catalytic layer is presented in Fig. 1a. The water released by H_2 electrochemical oxidation is involved further in the anode compartment, inside the porous catalyst, in the conversion of the hydrocarbon by steam reforming. It results that both reactions can be self-sustained by each other without any additive at the inlet. Water molecules, generally being a waste of the high temperature fuel cell, are in this process valued as reactant for steam reforming. The other main advantage of GIR is a delocalisation of the high endothermicity of the reforming reaction on the whole volume of the anode, which considerably limits thermal gradients and mechanical stress of the cell. GIR operation, initially proposed for tubular cell configuration, can also be applied to planar designs as indicated in Fig. 1b. Using a gas diffuser, the fuel radiates as a laminar flow from the center of the cell to the perimeter, enabling gradual consumption of methane.

An intensive feasibility study of gradual internal reforming based on modelisation has already been carried out and reported

[13–15]. The feasibility has also been demonstrated experimentally [11,12].

Modeling was based on solving the conservation equations of mass, momentum, energy, species and electric current using a finite volume approach on 2D grids of arbitrary topology. Simulations using the CFD-Ace software package allowed the calculation of partial pressure distributions, current density and electronic and ionic phase potentials in the anode part (i.e. gas channel and electrodes). A detailed thermodynamic post-processing analysis was carried out, taking into account the Boudouard reaction and the methane cracking reaction, so as to predict the carbon formation boundary for methane-fuelled SOFCs. Firstly it was demonstrated that the cooling effect due to the high endothermicity of the reforming reaction in direct internal reforming (DIR) has completely disappeared in GIR. Secondly it was proved that electrochemical performances are higher in GIR than in DIR. Nevertheless it is also clear that GIR implies most important risks of carbon formation. To cope with this drawback a new geometry configuration has been developed. In this case, a catalyst layer that promotes methane reforming is added. It should be noted that this catalyst layer does not promote carbon formation. With a catalyst layer thickness of $750 \mu\text{m}$ and a kinetic reforming rate 10 times higher than the reforming rate in the cermet, carbon deposition is not thermodynamically favoured throughout the length of the SOFC.

Finally, direct operation with pure methane, without additives in the fuel such as O_2 , CO_2 , H_2O or carrier gas, will lead to substantial technological simplification of the systems and also important cost reductions.

2. Experimental

2.1. Cell configuration

The configuration of the cell tested in this study is identical as that presented in a previous paper [12]. It was built-up from 8 mol% yttria-stabilized zirconia (YSZ-TOSOH) supporting electrolyte ($\sim 1 \text{ mm}$ thick). Additional informations are provided in the following sections.

2.1.1. Cathode side

The cathode was consisted of $\text{La}_{0.8}\text{Sr}_{0.2}\text{MnO}_{3-x}$ (LSM, $\sim 60 \mu\text{m}$ thick), deposited by pulverization of an aerosol containing ethylene glycol in several steps alternated with drying steps in an oven heated at 100°C . Current collection was provided by a gold grid pressed onto the electrode surface. The cathode compartment was fed with air (flow rate = 100 standard cubic centimetres per minute (SCCM)).

2.1.2. Anode side

The anode was consisted of a Ni-YSZ cermet (YSZ, $\sim 70 \mu\text{m}$ thick). At the top of it, a catalyst layer of about $500 \mu\text{m}$ thick consisted

of 0.1 wt.% Ir impregnated ceria (CeO_2), was deposited onto this conventional cell. Both layers were deposited by pulverization of an aerosol using the same conditions as for the cathode.

Ceria powder was impregnated by Ir using iridium acetylacetonate $[\text{CH}_3\text{COCH}=\text{C}(\text{O}^-)\text{CH}_3]_3\text{-Ir}$. Current collectors were realised using an original design. The main issue concerning current collection in this cell was that direct contact between platinum and methane had to be avoided absolutely because platinum yielded carbon cracking. Accordingly, platinum collectors were inserted into the electrolyte surface as $200\ \mu\text{m}$ wires in a $200\ \mu\text{m}$ groove, and fixed with platinum paint. In the following, these current collectors will be referred to as internal collectors. After deposition of the cermet anode, platinum collectors were connected to gold coils using a gold annulus, gold and alumina paste. This specific configuration enables current collection without physical contact between platinum and methane.

The anode compartment could be fed with various $\text{Ar}/\text{H}_2/\text{CH}_4/\text{H}_2\text{O}$ mixtures with various flow rates, obtained using specific mass flowmeters and steam controller. The gas used were methane G20 (air liquide), hydrogen MESSER, argon Ar1 (air liquide). In the following sections, the steam to carbon ratio (S/C) will be denoted as $R = [\text{H}_2\text{O}]/[\text{CH}_4]$.

2.1.3. Current and gas management

The cell was then inserted in a specific three atmospheres characterisation set-up. Sealing between compartments was achieved using gold wires.

All the gas lines at the inlet and outlet of the anodic side were heated at $T \geq 333\ \text{K}$ with heating coils to prevent from steam condensation.

The third compartment was fed with neutral gas (Ar). A platinum wire was placed in a groove deepen all around the electrolyte and intimately connected to it with gold paste to get a stable electrical potential which allows three-electrodes measurements. This set-up was essential to separate and identify anodic and cathodic overpotentials during operation. Two gold wires were connected to the anodic collector and two others to the cathodic one. One was used to measure the electrode potential, the other the current so that the ohmic losses due to the set-up, and especially heated gold coils, were automatically subtracted without further treatment. In other words, the set-up is electrically transparent. All the measurements were realised with the furnace tempera-

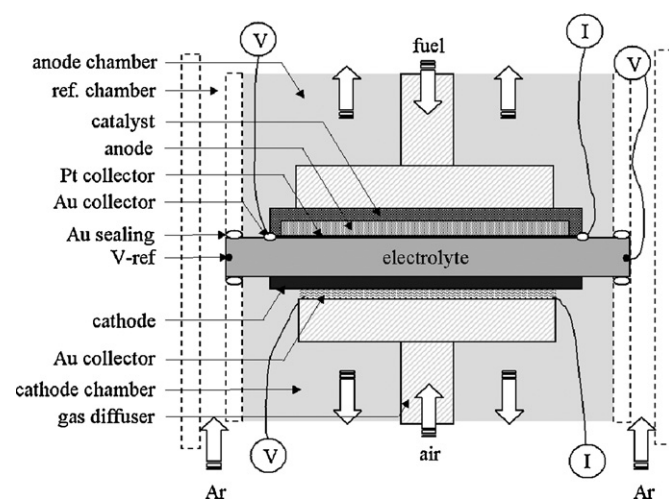


Fig. 2. Sketch of the three atmospheres experimental set-up used to characterised the cell.

ture set at $900\ ^\circ\text{C}$. A sketch of the experimental set-up is given in Fig. 2.

2.2. Characterisation

Electrical and electrochemical properties were analyzed using coupled SOLARTRON SI1250 Frequency Response Analyzer and SI1287 Electrochemical Interface. SEM micrographs were realised using a LEO S440 scanning electron microscope.

The outlet anodic gas phase was analyzed using on-line gas phase chromatograph (HP6890 GC System). Steam was condensed between the anode and the chromatograph.

3. Results and discussion

3.1. Microstructural characterisation of cell components and internal collector

The cell components have been characterised by scanning electron microscopy. SEM micrographs of anode and cathode are presented in Fig. 3. Parts (a) and (b) are polished cross-sections,

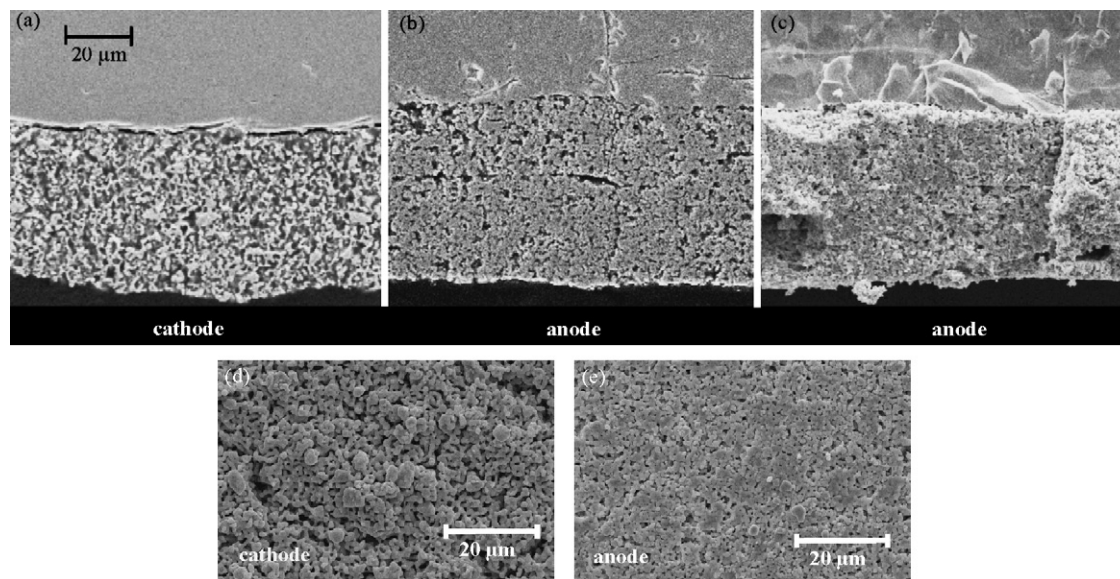


Fig. 3. SEM micrographs of polished cross-sections and surfaces of anode and cathode.

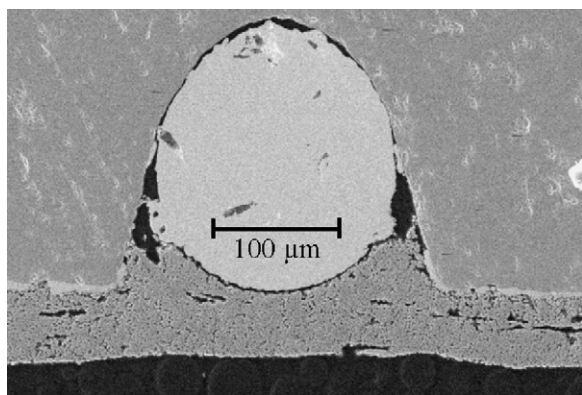


Fig. 4. SEM micrographs of a polished cross-section of the anode showing the internal collecting system.

part (c) is a fracture. The images first confirm the high relative density of the electrolyte. The cathode is about $60\ \mu\text{m}$ thick and present homogeneous microstructure. The delamination from the electrolyte surface observed in Fig. 3a might be due to the sample's preparation (polishing) rather than ageing during operation. The anode is about $70\ \mu\text{m}$ thick and present good adhesion onto the electrolyte surface. In some places, the interface between the successive anode layers deposited by spray are visible (Fig. 3b). It results that the deposition route and final microstructure of the electrode could be improved.

Fig. 3d and e present SEM micrographs of the electrodes surfaces. For both cathode and anode, the microstructure is porous, homogeneous and free from cracks. The layers were highly resistant to mechanical strains (scratch with spatula). The microstructure of the catalyst layer is described elsewhere [12].

Collecting is one of the most critical issue in solid oxide fuel cells. Platinum is generally used. However, when hydrocarbons are involved, the problem is even more complicated. An original collecting system then had to be designed for this fuel cell to be operated with methane. The morphology of the collecting system is presented in the micrograph of Fig. 4. The polished cross-section image show the section of the $200\ \mu\text{m}$ platinum wire inserted in the electrolyte and covered by the cermet anode. Using this system, electrons are collected at the internal face of the anode, which require a good percolation of metallic nickel grains in the cermet. This concept was first validated on symmetrical cells by AC impedance spectroscopy at OCV. The measurements analysis indicated that collecting was identical whether the collector was a grid pressed onto the anode surface or the internal collecting system. Polarisation resistance was almost identical in both configurations. The high melting point of platinum ($1768\ ^\circ\text{C}$) allows the cermet to be sintered at $1350\ ^\circ\text{C}$ with the collector inserted without melting, diffusion or degradation. This would be impossible with gold collectors (m.p. of $1064\ ^\circ\text{C}$). Moreover, platinum is protected from the direct contact with methane by anode and catalyst layers (double physical and catalytic barrier).

3.2. Electrical/electrochemical characterisation

The three atmospheres—three probe original set-ups used allows specific measurements of both electrode reactions separately. Anode and cathode AC impedance spectra recorded at OCV after 24 h equilibration time in $10\% \text{H}_2$ diluted in Ar at $900\ ^\circ\text{C}$ are presented in Fig. 5. Each spectra consists of a well defined single circle arc and a significant inductive effect at high frequency. The polarisation resistance of the cathode is higher than that of the anode. Nevertheless, we have demonstrated that the cathode was activated under polarisation, so that resistances for both electrodes

were comparable under operation [12]. Thanks to this observation, we assumed that modifications of the global polarisation resistance under load conditions during long-term experiments (see after), were mainly due to the anode. Part (b) of Fig. 5 shows that the algebraic sum of separated spectra correspond very accurately to the experimental spectra of the complete cell, which validate the three atmosphere—three probe measurement set-up. Unfortunately, probably due to small leaks at gold wire gaskets, this configuration did not work anymore for the following experiments.

3.3. Cell testing

Because of the expected low performances of the cell due in particular to thick supporting electrolyte and non-optimised electrodes, the cell operation temperature was fixed to $900\ ^\circ\text{C}$ in order to get sufficient current to maintain the gradual internal reforming process, according to our simulations [15] and to the observations of Lin et al. [2].

The cermet anode was reduced in pure H_2 at $900\ ^\circ\text{C}$. The polarisation curves under different atmospheres (Ar/ H_2 : 85/15% and $\text{CH}_4/\text{H}_2\text{O}/\text{Ar}$: 20/5/75%) are presented in Fig. 6. For the case of CH_4 , the ratio $R = [\text{H}_2\text{O}]/[\text{CH}_4]$ is lower than 1, which represents gradual internal reforming conditions. In other words, the steam quantity at the inlet of the cell is not sufficient to thoroughly and directly operate steam reforming reaction. The $V-i$ curves were recorded with a potential scanning rate of $10\ \text{mV min}^{-1}$, leading to about 2 h for one curve. In these conditions, no degradation or carbon deposition was observed.

The open circuit voltage of about $1.07\ \text{V}$ under H_2 was almost independent from the proportion of carrier gas in the fuel. On the contrary, the OCV of $1.25\ \text{V}$ under diluted and humidified methane increased when the proportion of water was lowered [12] (i.e. for increasingly GIR conditions). These observations are in agreement with thermodynamic predictions, according to the Nernst law

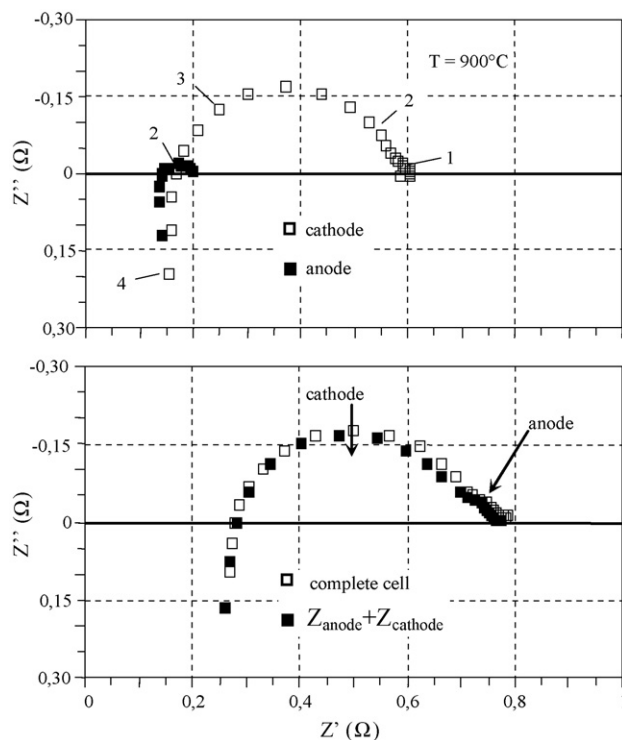


Fig. 5. (a) AC impedance spectra recorded at OCV showing anode and cathode polarisation; (b) AC impedance spectra recorded at OCV of the complete cell; closed symbols represent the sum of cathode and anode impedances.

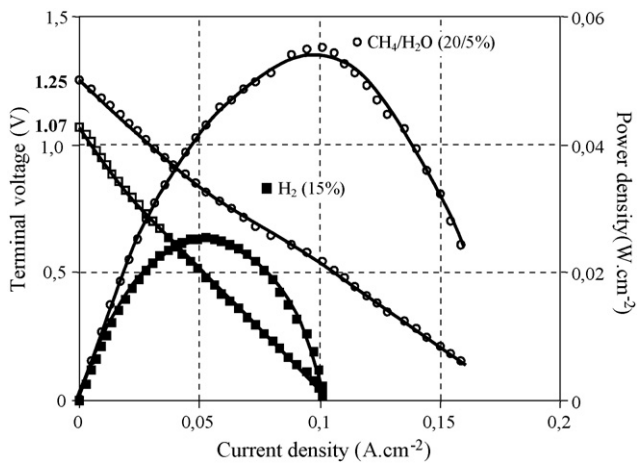


Fig. 6. Steady state $V-i$ curves obtained at 900°C in diluted H_2 and in $\text{CH}_4/\text{H}_2\text{O}$ with a total flow rate of 100 SCCM (argon was used as carrier gas).

[1,12,14]:

$$E = E^\circ + \frac{RT}{8F} \ln \frac{(P_{\text{CH}_4})_a (P_{\text{O}_2})_c^2}{(P_{\text{H}_2\text{O}})_a^2 (P_{\text{CO}_2})_a} \quad (2)$$

Note that in the simplified approach mentioned above, methane is considered to react directly in CO_2 and H_2O . The Nernst law refers to the following reaction:



Note also that the presence of the catalyst layer would modify the thermodynamic behavior of the cell.

These higher OCV yielded better performances under $\text{CH}_4/\text{H}_2\text{O}$ than in H_2 . The current density at max power were about 0.1 and 0.05 mA cm^{-2} for $V \sim 0.5 \text{ V}$. As expected, such a low current density is directly related to the electrolyte thickness, but it will be sufficient to demonstrate the ability of this cell to operate in pure and dry methane without carbon deposition. The curvature of the polarisation curves is due to the activation of the cathode under load conditions yielding a decrease of cathodic overpotential. This behavior was reported and analyzed elsewhere [12].

Several tests were realised in order to determine the optimal operation conditions of the cell regarding in particular carbon deposition. Total and partial flow rates of methane were first adjusted to determine the best compromise between fuel utilisation and per-

formances. A sufficient quantity of methane is needed to obtain a significant power density and subsequent hydrogen and water production to maintain the gradual internal reforming process. However, a too high methane flow rate will yield a low fuel utilisation rate. Experimental details are presented in Fig. 7a for a total flow rate of 100 SCCM with Ar as carrier gas. The steam proportion was kept at 2%. For methane proportions higher than 4%, current density tends to a maximum, which indicates that higher quantities yield lower fuel utilisation. For the following, methane flow rate was then fixed to 4 SCCM. In these conditions, a faradic efficiency calculation gave a value of about 30%.

In these conditions, the cell potential for middle-term operation tests was determined similarly (Fig. 7b). It was found that 0.6 V led to the best operation stability and yielded sufficient current density to maintain GIR operation.

This set of parameters was applied for the middle-term experiments in dry methane. In order to initiate the gradual internal reforming process, the cell was first operated with 15% H_2 in argon, with a total flow rate of 100 SCCM. This step is essential to begin the release of water molecules from the anode. After 1 h, when steady state operation was obtained, the atmosphere was suddenly switched to pure CH_4 with a total flow rate of 4 SCCM (0.24 L h^{-1}), which represent an optimal utilisation rate of the fuel (see Fig. 7). The anode reaction being initiated and maintained through the gas flow on the electrode compartment, steam flows from the anode to the catalyst maintaining the reforming reaction. Catalytic and electrochemical reactions are thus separated and self-sustained by each other through the gradual internal reforming process, the catalyst providing a double protection layer (diffusion barrier and catalytic filter), as already mentioned by Zhan and Barnett for iso-octane partial oxidation [4].

The operation of the cell was analyzed during 120 h. An impedance spectra (under load conditions at $V = 0.6 \text{ V}$) was recorded each 4 h during this period of time, and the outlet gas phase was analyzed by chromatography. Note that water, condensed before the chromatograph, was not quantified.

Impedance spectra were made of a single circle arc and a small inductive loop at high frequency. Electrical parameters were extracted by least-squares refinement procedures. The simplest physically meaning electrical circuit was consisted of serial inductance and resistance connected with R//CPE circuit (CPE is a constant phase element). Cyclic refinement provided several electrical parameters: $R_s, R_p, R_t, C, p,$ and w_0 for serial, parallel and total resistances, capacitance, homogeneity (distribution of relaxation times) and relaxation frequency, respectively. They gave informa-

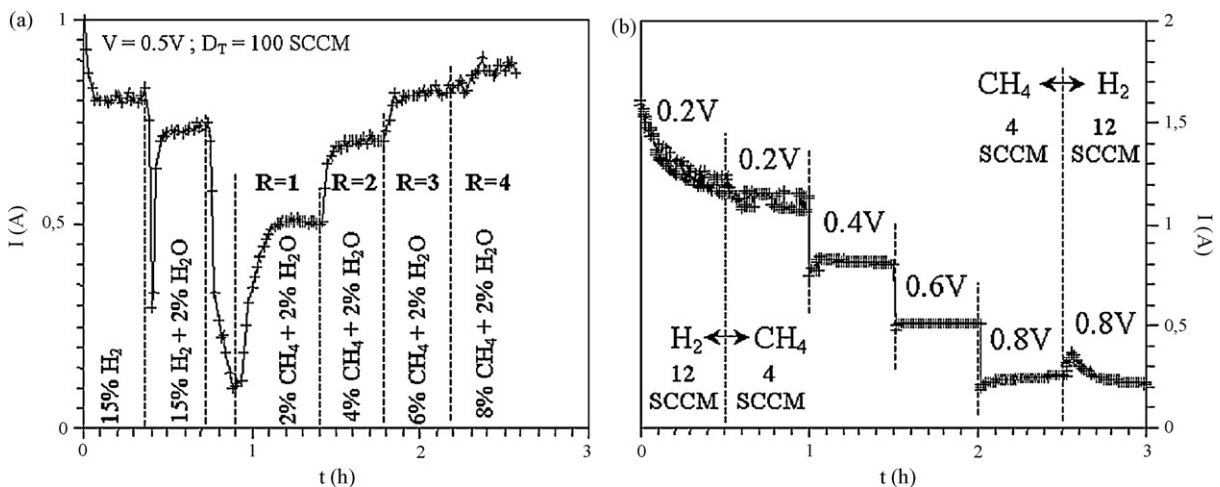


Fig. 7. (a) Evolution of the current as a function of time for different reforming conditions from direct internal reforming ($R = 1$) to gradual internal reforming ($R = 4$); cell was operated at $V = 0.5 \text{ V}$ with a total flow rate of 100 SCCM; (b) evolution of the current in pure CH_4 as a function of cell voltage.

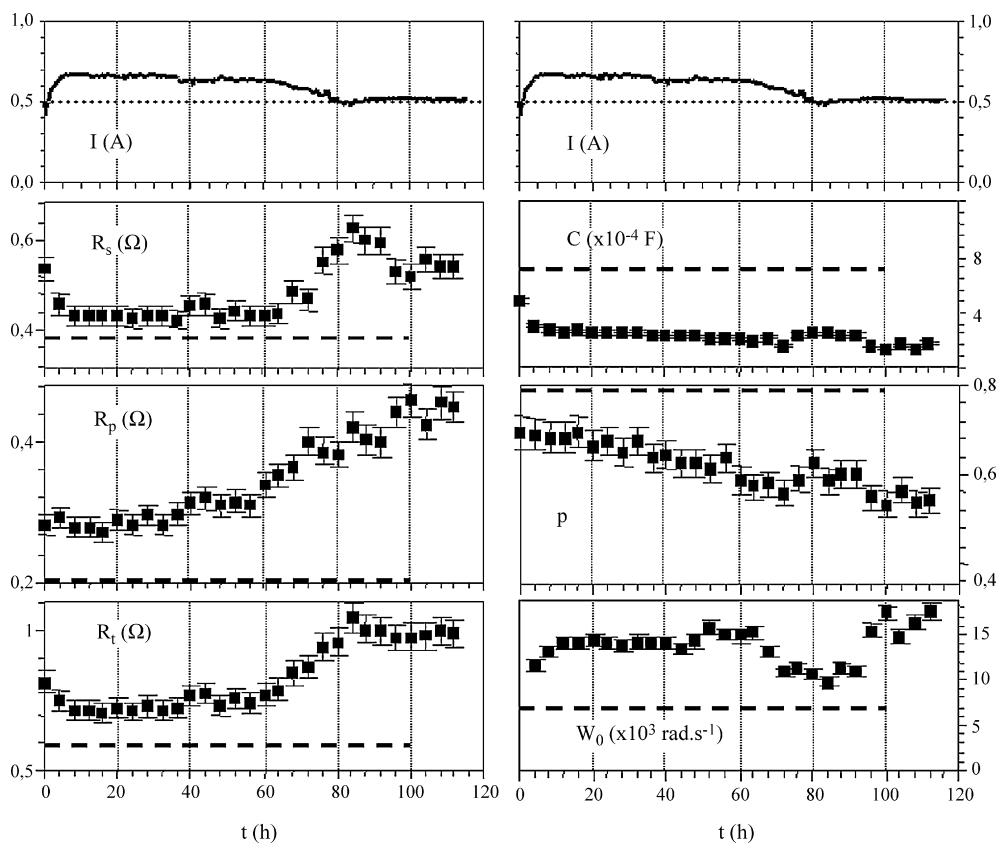


Fig. 8. Evolution as a function of time of the electrical and electrochemical parameters of the cell determined by least-squares refinement using a R//CPE electrical circuit; the cell was operated at $V = 0.6\text{ V}$ in pure CH_4 with a total flow rate of 4 SCCM; dashed line represents the levels measured at OCV in diluted H_2 at 900°C .

tions concerning the electrolyte apparent resistance (including geometric effects), and the global electrode process. The evolution of these parameters as a function of time is presented in Fig. 8 and correlated to the evolution of the current. First, the current is stable for about 20 h before stabilisation at a lower level for another 40 h. All the electrical parameters show similar evolutions. The analysis of the resistive components of the electrical circuit (R_s and R_p) indicates that both the apparent electrolyte resistance and the electrode global polarisation resistance increase.

The parameter p , giving indications on the homogeneity of the electrode reaction ($p = 1$ for homogeneous process, i.e. pure capacitor with no distribution of relaxation times) decreases gradually indicating a slow but steady degradation of the electrode probably due to mechanical stresses. The abrupt evolution of all parameters at about 60 h can be explained by partial delamination of the anode, resulting in a relaxation of the stress endured by the cell yielding subsequent stabilisation. After stabilisation of the current, all the parameters still evolve, indicating that the cell would have been further deteriorated for a longer experiment. Partial delamination of the anode affected the performances of the cell (lower current), leading to lower steam release from the anode to the catalyst. The consequence was a lower methane conversion. This analysis is reinforced by chromatographic measurements presented in Fig. 9 and compared to the current as a function of time. The decrease of the performances was accompanied by a respective increase and decrease of methane and CO concentrations. In other words, it is most probable that the conversion of methane introduced at the anode side decreased, explaining lower currents, rather than other phenomenon like carbon deposition. Indeed, after preliminary operations tests, Ar containing 10 ppm O_2 was flown at the anode side with a flow rate of 100 SCCM. Air was flown at the cath-

ode with the same flow rate. Several chromatograms were recorded by gas phase chromatography for 24 h. No C oxidation products (CO or CO_2) were detected. The same test was realised after the long-term experiment of 120 h, and followed by a test of air flow at the anode, with the same flow rate of 100 SCCM. Again, no carbon oxides were detected. These observations indicate that the degradation observed was not a consequence of carbon cracking or even

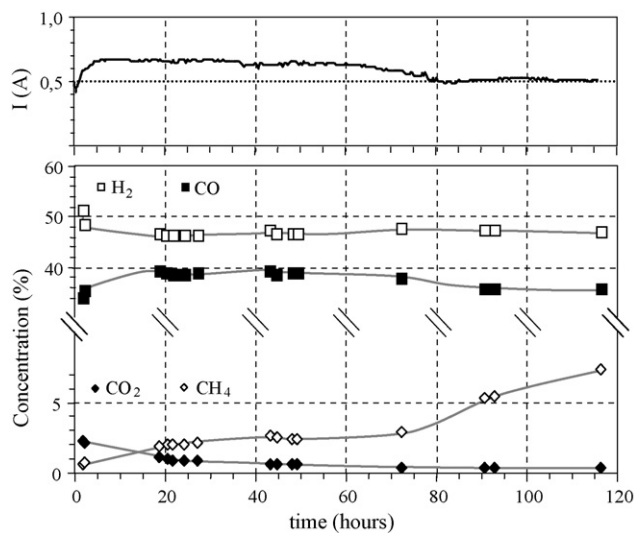


Fig. 9. Evolution as a function of time of the anodic gas phase composition compared to the current of the cell; the cell was operated at $V = 0.6\text{ V}$ in pure CH_4 with a total flow rate of 4 SCCM; dashed line represents the levels measured at OCV in diluted H_2 at 900°C .

more generally carbon deposition on the anode. This analysis is supported by electrochemical analysis provided in Fig. 8. The evolution of both polarisation (electrode process) and serial (electrolyte resistance) resistances demonstrate that the deactivation of the cell is mainly due to delamination than carbon deposition since the serial resistance is directly related to the anode to electrolyte contact interface.

Fig. 9 also indicates that H₂ and CO are the major products of the anode reaction, as already reported in similar conditions [2], H₂ being of course partly consummated. This element supports the assumption that steam reforming is the main methane conversion reaction occurring in the catalytic layer, and consequently that it can only be fed from water molecules released by electrochemical oxidation of hydrogen produced. In other words, the operation of the cell is well explained by the gradual internal reforming process associated with the separation of electrochemistry and heterogeneous catalysis, as proposed in the introduction. On the contrary, CO₂ concentration is low in the exhaust gas phase.

After dismantle of the experimental set-up, the anode side was found free from coke but also completely broken probably because of the oxidation tests.

Finally, this fuel cell was operated more than 200 h (120 consecutive) under pure and dry methane with an almost constant current. Analysis of experimental data presented in this paper show that the hand-made cell was clearly not optimised. Attention has now to be paid on the elaboration of all cell components in order to extend the life-time. It is difficult to distinguish whether this cell had intrinsic low life-time or the degradations observed were related to the use of pure methane.

4. Conclusion

A SOFC was operated in pure methane for about 200 h at 900 °C. No carbon deposition was detected. As mentioned in the literature [2], the higher the operating temperature, the higher has to

be the critical current density needed to avoid coke formation for conventional cells. In this study, the operation was undertaken at 900 °C because our cell gave very low current density. Nevertheless, with current density as low as 0.1 A cm⁻², no important decrease of performances or coke formation was detected. This behavior is due to the addition of a specific catalytic layer onto the anode, pre-treatment in H₂ to initiate the GIR process, and selection of optimal operation conditions regarding in particular cell potential, fuel flow rate and fuel utilisation rate.

The experimental results obtained here on the light of the results of modelisation already reported, and of the data available in the literature, underline that coking in direct hydrocarbon SOFC has to be considered with both thermodynamic and kinetic aspects. In the conditions reported here, steam released at the cermet is likely to feed steam reforming rather than helping coke removal. In other words, the catalytic layer acts against coking from thermodynamic and kinetic aspects.

References

- [1] S. McIntosh, R.J. Gorte, *Chem. Rev.* 104 (2004) 4845–4865.
- [2] Y. Lin, Z. Zhan, S.A. Barnett, *Solid State Ionics* 176 (2005) 1827–1835.
- [3] Z. Zhan, S.A. Barnett, *Science* 308 (2005) 844–847.
- [4] Z. Zhan, S.A. Barnett, *J. Power Sources* 155 (2006) 353–357.
- [5] P.K. Cheekatamarla, C.M. Finnerty, J. Cai, *Int. J. Hydrogen Energy* 33 (2008) 1853–1858.
- [6] S. Park, J.M. Vohs, R.J. Gorte, *Nature* 404 (2000) 265–267.
- [7] S. Park, R. Craciun, J.M. Vohs, R.J. Gorte, *J. Electrochem. Soc.* 146 (1999) 3603–3605.
- [8] H. Kim, S. Park, J.M. Vohs, R.J. Gorte, *J. Electrochem. Soc.* 148 (2001) A693.
- [9] H. He, Y. Huang, J.M. Vohs, R.J. Gorte, *Solid State Ionics* 175 (2004) 171–176.
- [10] P. Vernoux, J. Guindet, M. Kleitz, *J. Electrochem. Soc.* 145 (10) (1998) 3487–3491.
- [11] S. Georges, G. Parrou, M. Hénault, J. Fouletier, *Solid State Ionics* 177 (2006) 2109–2112.
- [12] J.M. Klein, M. Hénault, P. Gélin, Y. Bultel, S. Georges, *Electrochem. Solid State Lett.* 11 (2008) B144–B147.
- [13] J.M. Klein, Y. Bultel, S. Georges, *J. Electrochem. Soc.* 155 (4) (2008) B333–B339.
- [14] J.M. Klein, Y. Bultel, S. Georges, M. Pons, *Chem. Eng. Sc.* 62 (2007) 1636–1649.
- [15] J.M. Klein, Y. Bultel, S. Georges, M. Pons, *Electrochem. Soc. Trans.* 7 (1) (2007) 1419.